Bioorganic & Medicinal Chemistry Letters 18 (2008) 3545–3550

Contents lists available at ScienceDirect

Bioorganic & Medicinal Chemistry Letters

journal homepage: www.elsevier.com/locate/bmcl

Design, synthesis, and structure–activity relationships of piperidine and dehydropiperidine carboxylic acids as novel, potent dual PPARα/γ agonists

Xiang-Yang Ye [a,*], Yi-Xin Li [b], Dennis Farrelly [c], Neil Flynn [c], Liqun Gu [c], Kenneth T. Locke [d], Jonathan Lippy [d], Kevin O'Malley [d], Celeste Twamley [d], Litao Zhang [d], Denis E. Ryono [a], Robert Zahler [a], Narayanan Hariharan [c], Peter T. W. Cheng [a,*]

[a] Metabolic Diseases Chemistry, Bristol-Myers Squibb R&D, PO Box 5400, Princeton, NJ 08543-5400, USA
[b] Discovery Analytical Sciences, Bristol-Myers Squibb R&D, PO Box 5400, Princeton, NJ 08543-5400, USA
[c] Metabolic Diseases Biology, Bristol-Myers Squibb R&D, PO Box 5400, Princeton, NJ 08543-5400, USA
[d] Lead Evaluation, Bristol-Myers Squibb R&D, PO Box 5400, Princeton, NJ 08543-5400, USA

ARTICLE INFO

Article history:
Received 21 March 2008
Revised 1 May 2008
Accepted 2 May 2008
Available online 6 May 2008

Keywords:
Peroxisome proliferator-activated receptors
Piperidine and dehydropiperidine carboxylic acids
Structure–activity relationships
Dual agonists

ABSTRACT

Several series of substituted dehydropiperidine and piperidine-4-carboxylic acid analogs have been designed and synthesized as novel, potent dual PPARα/γ agonists. The SAR of these series of analogs is discussed. A rare double bond migration occurred during the basic hydrolysis of the α,β-unsaturated dehydropiperidine esters **12**, and the structures of the migration products were confirmed through a series of 2D NMR experiments.

Peroxisome proliferator-activated receptors (PPARs) belong to a nuclear hormone receptor superfamily which act as transcription factors in the regulation of genes involved in glucose and lipid homeostasis.[1] Three PPAR subtypes have been identified: PPARα, PPARγ and PPARδ. PPARα is highly expressed in liver, but is also present in heart, kidney, and muscle, and regulates the transcription of numerous genes encoding proteins involved in lipid metabolism.[2] Currently marketed PPARα agonists are the fibrate class of drugs (including fenofibrate[3] and gemfibrozil[4]), which elevate HDL levels and lower triglyceride and LDL levels. PPARγ is predominantly expressed in adipose tissue and regulates insulin sensitivity, glucose and fatty acid utilization as well as adipocyte differentiation.[5] Currently marketed drugs targeting PPARγ are rosiglitazone[6] and pioglitazone,[7] both for the treatment of type 2 diabetes. We have recently reported the design and synthesis of Muraglitazar (**1**, Fig. 1), a dual PPARα/γ agonist which has shown excellent efficacy in animal models of type 2 diabetes and the associated dyslipidemia as well as in human clinical trial.[8] Starting from the oxybenzyl-glycine template exemplified by **1**, several series of potent, conformationally constrained dual PPARα/γ agonists have been designed and synthesized.[9] From this effort, a series of 3-benzyl-4-carboxy-pyrrolidines, exemplified by compound **2**, was identified which has good activity both in vitro and in vivo.[10] To further explore the scope of the SAR of this pyrrolidine acid series, we decided to investigate the effect of expanding the pyrrolidine ring of **2** into the corresponding piperidine acids (Fig. 2). This paper focuses on the design, synthesis, and SAR of various piperidine/dehydropiperidine carboxylic acid analogs as dual PPARα/γ agonists.

Chemistry. Based on results from the pyrrolidine acid series and preliminary modeling studies, we focused our initial efforts on the dehydropiperidine acid analogs **3** (with both 1,4- and 1,3-oxybenzyl substituents). These compounds should be readily derived from dehydropiperidine intermediates **4** (Scheme 1). Our initial efforts to synthesize **4** (especially where $m = 1$) were unsuccessful. For instance, in one approach, the enolate of *N*-Boc-4-oxopiperidine was successfully alkylated with 4-methoxybenzyl bromide; however, subsequent attempts to convert the carbonyl group into the C-4 carboxylic acid (via carbonylation of the enol triflate of the ketone) were unsuccessful. Recently, Bellina[11] reported that vinyl nonaflates (derived from β-keto esters) act as excellent electrophiles in palladium-catalyzed cross-coupling reactions using a variety of organozinc halides. This report encouraged us to apply this approach to the successful synthesis of **4** outlined in Scheme 1. Vinyl nonaflate **6** was easily obtained from *N*-benzyl-3-oxopiperidine-4-carboxylate by treatment with base (NaH or KHMDS),

* Corresponding authors. Tel.: +1 609 818 4130; fax: +1 609 818 3460.
E-mail addresses: xiang-yang.ye@bms.com (X.-Y. Ye), peter.t.cheng@bms.com (P.T.W. Cheng).

0960-894X/$ - see front matter © 2008 Elsevier Ltd. All rights reserved.
doi:10.1016/j.bmcl.2008.05.014

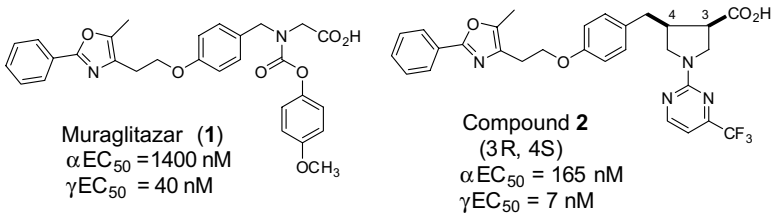

Figure 1. Structure of Muraglitazar (**1**) and the related pyrrolidine-acid analog **2**.

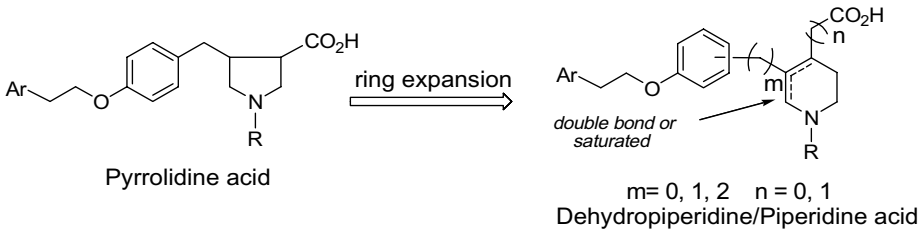

Figure 2. The design of piperidine/dehydropiperidine carboxylic acids as dual PPARα/γ agonists.

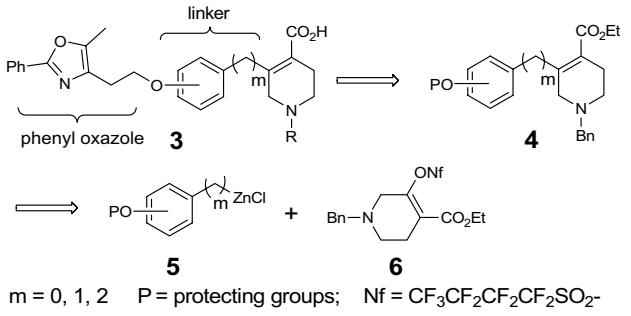

Scheme 1. Retrosynthetic analysis of dehydropiperidine-4-carboxylate **3**.

followed by nonafluoro-1-butanesulfonyl fluoride (Nf-F). Without further purification, nonaflate **6** was reacted with zinc halides **5** in the presence of catalytic $Pd(dba)_2$/dppf to afford **4** in 70–80% yield in two steps. This convergent approach allowed us to quickly access the desired intermediates **4** in both the 1,3- and 1,4-oxyphenyl series (bearing a variety of carbon linkages where $m = 0$, 1 or 2) by simply altering the organozinc halides **5**. Organozinc reagents **5** which were not commercially available were prepared either: (1) in situ via the exchange of the Grignard reagent or organolithium with $ZnCl_2$ or (2) from reaction of the alkyl or aryl halide with activated zinc.

To illustrate the versatility of this synthetic route, the synthesis of the 1,3-oxybenzylpiperidine acid analogs **13** is shown in Scheme 2. The Pd-catalyzed cross-coupling reaction of vinyl nonaflate **7**[11] and 3-(*tert*-butyldimethylsilyloxy)benzylzinc chloride[12] afforded **8** in 75% yield. Deprotection of the *N*-benzyl group with α-chloroethyl chloroformate[13] was achieved with concomitant desilylation of the phenol. *N*-Boc reprotection of the piperidine afforded phenol **9**, which was alkylated with mesylate **10** and then deprotected to give the key intermediate secondary amine **11**, which enabled us to quickly explore SAR at the dehydropiperidine nitrogen. Intermediates **11** were treated with alkyl/aryl chloroformates to give carbamates, or with substituted 2-chloropyrimidines to form *N*-pyrimidines. The desired carboxylic acid analogs **13** were obtained via acid-mediated ester hydrolysis.

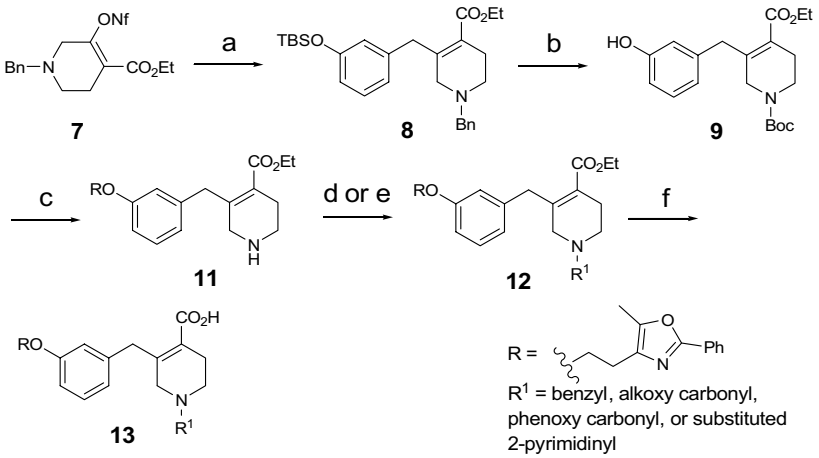

Scheme 2. The synthesis of 1,3-oxybenzyl dehydropiperidine analogs **13**. Reagents and conditions: (a) 3-(*tert*-butyldimethylsilyloxy)benzylzinc chloride, $Pd(dba)_2$, dppf, THF, 65 °C, 12 h, 75%; (b) (i) α-chloroethyl chloroformate, 50 °C, 1 h; then MeOH; (ii) Boc_2O, THF-$NaHCO_3$ (aq), 2 h, 72% (two steps); (c) (i) 2-(5-methyl-2-phenyloxazol-4-yl)ethyl methanesulfonate (**10**), K_2CO_3, CH_3CN, 90 °C, 12 h, 90%; (ii) 4 N HCl in dioxane, MeOH, rt, 5 h, 95%; (d) THF–H_2O, $NaHCO_3$, alkyl or aryl chloroformate, 1 h, 90–95%; (e) 2-chloropyrimidine, *i*-Pr_2NEt, toluene, 100 °C, 3 h, 85–90%; (f) 15% HCl in HOAc, sealed tube, 100 °C, 8 h, 70–80%.

Analogs with different linkers to the dehydropiperidine ring (e.g. 1,4-oxyphenethyl [**14**], 1,4-oxyphenyl [**15**], 1,3-oxyphenyl [**16**] and 1,4-oxybenzyl [**17**]) were also readily synthesized using this general route, as various organozinc chlorides could readily be substituted for the exemplified 3-(*tert*-butyldimethylsiloxy) benzylzinc chloride shown in Scheme 2. In all cases, the syntheses worked well and multiple analogs from each of these series (*N*-benzyl, *N*-alkoxycarbonyl, *N*-pyrimidinyl) were prepared (Fig. 3).

We then explored the synthesis of the corresponding piperidine acid analogs. This was unexpectedly problematic, as hydrogenation of C=C bond of the fully elaborated tetrasubstituted α,β-unsaturated esters (i.e. **12**) was accompanied by varying degrees of reduction of the phenyloxazole moiety (to the cyclohexyloxazole). Therefore, we needed to address the reduction of the C=C bond prior to the coupling with the phenyloxazole 'left-hand-side'. The successful alternative synthesis for these piperidine acid analogs is shown in Scheme 3, and is exemplified for the 1,3-oxyphenyl series; analogs **22**–**25** were also synthesized using this general route.[14]

Based on previous experience in the pyrrolidine acid series, increasing the distance between the piperidine ring and the carboxylic acid might improve both PPAR binding affinity and functional activity. Therefore, the homologated dehydropiperidine carboxylic acid analogs **31** and their corresponding piperidine analogs **32** were synthesized as shown in Scheme 4.[15] The key sequence is the conversion of **27** to **28**, which involves the palladium-catalyzed CO carbonylation of the allylic bromide derived from **27**.[16] The rest of the synthetic route is identical to Scheme 1. Piperidine analogs **32** were also synthesized using a combination of the chemistry shown in Schemes 2 and 3.

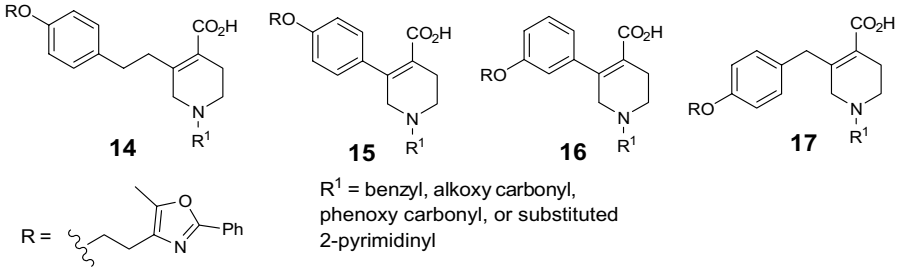

Figure 3. 1,4-Oxyphenethyl, 1,4-oxyphenyl, 1,3-oxyphenyl, and 1,4-oxybenzyl dehydropiperidine carboxylic acid analogs.

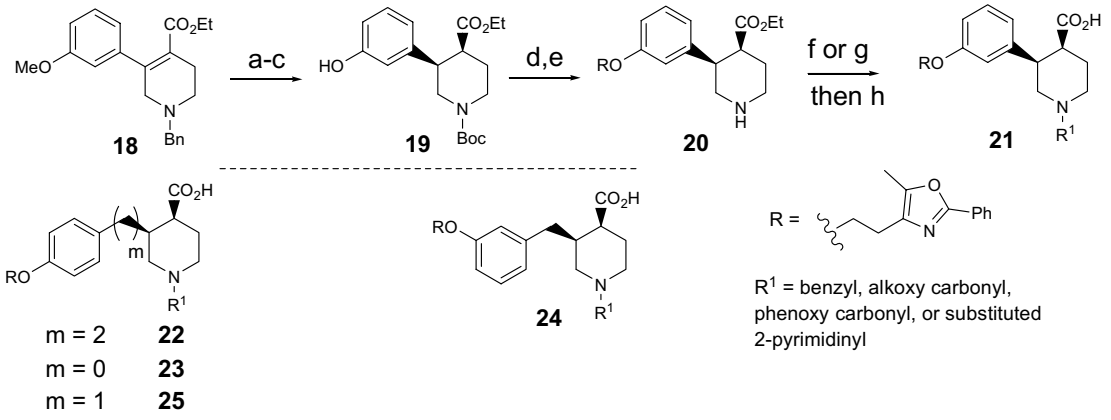

Scheme 3. The synthesis of piperidine carboxylic acids. Reagents and conditions: (a) 10% Pd-C, H_2 (80 psi), HOAc, overnight; (b) BBr_3 (3.5 equiv), CH_2Cl_2, −78 to 0 °C, 2 h; (c) Boc_2O, THF–H_2O, $NaHCO_3$, 2 h, 51% (three steps); (d) 2-(5-methyl-2-phenyloxazol-4-yl)ethanol (**26**), Bu_3P=CH–CN; toluene, 50 °C, 2 h, 95%; (e) AcCl/MeOH, 0 °C to rt, 5 h, 99%; (f) THF–H_2O, $NaHCO_3$, alkyl or aryl chloroformate, 1 h, 90–95%; (g) 2-chloropyrimidine, *i*-Pr_2NEt, toluene, 100 °C, 3 h, 85–90%; (h) 15% HCl in HOAc, sealed tube, 100 °C, 8 h, 70–80%.

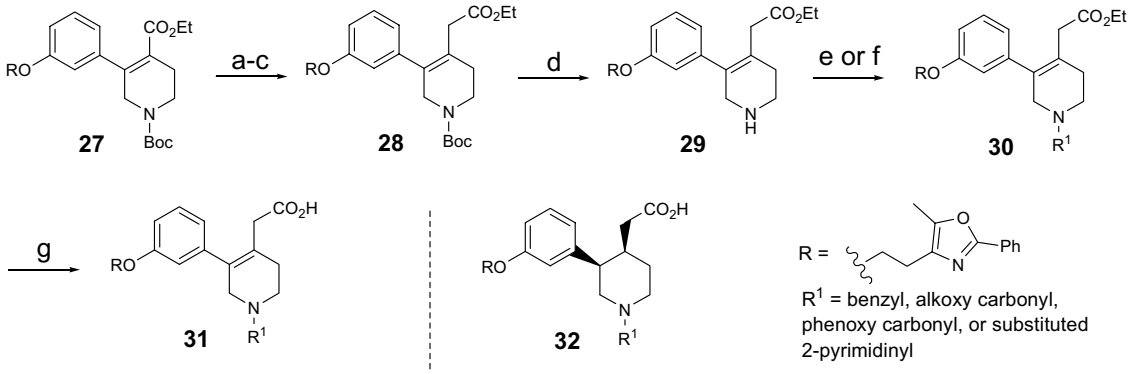

Scheme 4. The synthesis of homologated piperidine carboxylic acids. Reagents and conditions: (a) $LiAlH_4$, THF, −78 to 10 °C, 3 h, 95%; (b) PPh_3, CBr_4, CH_2Cl_2, 0 °C to rt, 2 h, 93%; (c) $Pd(PPh_3)_4$, $KHCO_3$, MeOH, CO (100 psi), rt, overnight, 61%; (d) AcCl/MeOH, 0 °C to rt, 5 h, 95%; (e) THF–H_2O, $NaHCO_3$, alkyl or aryl chloroformate, 1 h, 90–95%; (f) 2-chloropyrimidine, *i*-Pr_2NEt, toluene, 100 °C, 3 h, 85–90%; (g) 15% HCl in HOAc, sealed tube, 100 °C, 8 h, 70–80%.

In previous schemes, the final step of analog synthesis was acid-mediated ester hydrolysis. Under these conditions, the C=C bond of the α,β-unsaturated acid did not undergo migration (Scheme 2). However, due to the need for milder conditions required by more sensitive functionalities, we explored base-mediated hydrolysis (LiOH, THF–H_2O, rt) of the penultimate ethyl ester intermediate with analogs from the 1,3-oxybenzyl series **12**. Due to the sluggishness of the basic hydrolysis, three drops of methanol were added to accelerate the reaction, which then proceeded smoothly to completion. Surprisingly, the desired α,β-unsaturated acid **13** was isolated only as the minor product. The major product had the same molecular weight as **13**, but its ^{1}H NMR spectrum contained a new vinyl proton (δ 6.73); the possible structures were thus the C=C migration products **33** or **34** (both of which bear a vinyl proton). The ratio of the C=C migration product versus **13** varied from 4:1 to 6:1, depending on the structure of R^1.

A set of 2D NMR experiments were carried out on the C=C migration product from the hydrolysis of **12a** (R = -CO_2-*i*Bu). These studies enabled us to unequivocally assign each proton and carbon in this compound (Fig. 4)[17] and to unambiguously demonstrate that its structure corresponded to **33a** rather than **34** (R^1 = *i*-Bu–O–C(O)$^-$). In particular, the ^{1}H–^{13}C Heteronuclear Multiple Bond Connectivity (HMBC) analysis proved to be very useful in this structure determination. The most important correlations (as shown in Fig. 4) are: (1) the vinyl proton H-24 with the carbonyl C-29 and, (2) the benzylic H-22 with C-20, C-18, C-24, and C-28.

This unexpected base-mediated C=C bond migration from the α,β-unsaturated acid to the β,γ-unsaturated acid is rare. However, this result is in agreement with the previous work of Jacobsen,[18] in which a similar C=C migration occurred upon treatment of a dehydropiperidine 4-ester with benzylamine. Several analogs bearing the general structure **33** have been synthesized according to Scheme 5.

Results and discussion. Following the versatile synthetic schemes outlined above, we were able to quickly generate analogs which explored the optimal linker length between the phenyloxazole moiety and the dehydropiperidine/piperidine ring (m = 0–2), as well as the optimal substitution of the central oxyphenyl ring (1,3- vs 1,4-). The SAR at the piperidine ring was explored primarily by modification of substituents at the piperidine nitrogen, e.g. *N*-benzyl, *N*-alkoxycarbonyl, *N*-phenoxycarbonyl and *N*-pyrimidinyl. The PPARα and γ binding affinity as well as the transactivation (functional) data of these novel piperidine analogs are shown in Table 1.

In the 1,4-oxyaryldehydropiperidine acid series, the linker between the oxyaryl and the dehydropiperidine moieties clearly had a significant effect upon PPAR activity. Both PPARγ and α potency increased with increasing linker length m, e.g. the isobutyl carbamates **15a** (oxyphenyl linker; m = 0) versus **17a** (oxybenzyl linker; m = 1). With the oxyphenethyl analog **14a** (m = 2; αEC$_{50}$ 56 nM; γEC$_{50}$ 74 nM), the PPARγ potency was increased by another 15-fold relative to **17a** while PPARα potency was maintained, resulting in equivalent, potent agonist activity at PPARα and γ. The phenethyl linker may offer more flexibility (versus the benzyl or phenyl linkers) allowing these analogs to bind in the ligand-binding domains (LBDs) of both PPARα and γ. However, in the piperidine acid series, both the 1,3-oxybenzyl analog **25a** and 1,4-oxybenzyl analog **24a** (m = 1) show significantly less activity at PPAR.γ than at PPARα. Changing the linker length as in the dehydropiperidine series [e.g. for the 1,3-oxyphenyl analog **21a** (m = 0) and the 1,4-oxyphenethyl analog **22a** (m = 2)] did not result in compounds with equipotent activity at PPARα and γ. An alternative way to modulate PPARα/γ functional activity is to introduce flexibility to the location of the carboxylic acid. For instance, the 1,3-oxyphenyl dehydropiperidinyl acetic acid analogs **31a** and **31b** (where the 1,3-oxyphenyl group is directly attached to the dehydropiperidine ring, [i.e. m = 0] but the carboxymethyl group has flexibility of movement), are potent dual PPARα/γ agonists. The analogous piperidines **32a** and **32b** are much less active at both PPARα and γ. In the 1,3-oxybenzyl series, the dehydropiperidine **13b** (and to a lesser extent **13a**) shows good binding affinity but poor functional activity. Finally (and perhaps most significantly) the serendipitously discovered β, γ-unsaturated acid analogs (**33a**–**d**) generally showed excellent binding and functional activity at both PPARα and γ. Compounds **33a**–**d** are significantly more potent at PPARγ than the corresponding α, β-unsaturated acid analogs **13a**–**d**, and in the cases of **33a** and **33c**, also show significantly more potent PPARα activity.

Overall, the SAR from these series of piperidine and dehydropiperidine analogs shows that PPARα/γ binding affinity and functional activity can be modulated by: (a) varying the oxyphenyl substitution (1,3 vs 1,4 series); (b) the linker between the oxyphenyl and the piperidine ring (m = 0–2), (c) dehydropiperidine versus piperidines, and (d) the linker between the piperidine and the carboxylic acid. From the SAR exploration of various piperidine and dehydropiperidine series, analogs from the 1,3- oxyphenyl dehydropiperidines (**31a**, **b**), the 1,4- oxyphenethyl dehydropiperidines

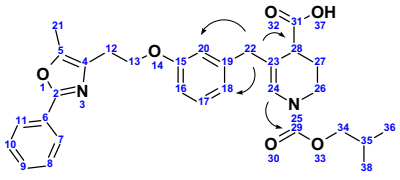

Figure 4. Some important HMBC correlations of **33a**.

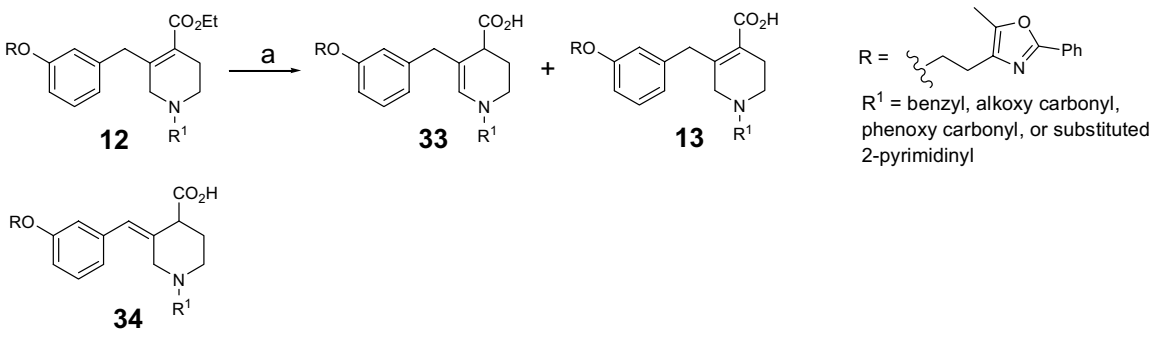

Scheme 5. Double bond migration in base-catalyzed ester hydrolysis. Reagents and conditions: (a) LiOH, THF–H_2O (2:1), trace amount of MeOH, rt, 3 h.

Table 1
In vitro activities of selected analogs at human PPARγ and α

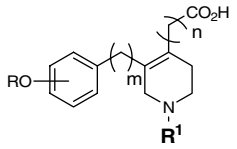

13 (m = 1, n = 0, 3'-OR)
14 (m = 2, n = 0, 4'-OR)
15 (m = 0, n = 0, 4'-OR)
16 (m = 0, n = 0, 3'-OR)
17 (m = 1, n = 0, 4'-OR)
31 (m = 0, n = 1, 3'-OR)

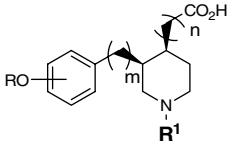

21 (m = 0, n = 0, 3'-OR)
22 (m = 2, n = 0, 4'-OR)
24 (m = 1, n = 0, 3'-OR)
25 (m = 1, n = 0, 4'-OR)
32 (m = 0, n = 1, 3'-OR)

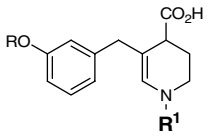

33

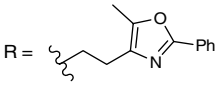

Compound	R^1	PPARγ binding IC_{50}(μM)[a]	HEK PPARγ EC_{50}(μM) (% activity @ 1 μM)[b]	PPARα binding IC_{50} (μM)[a]	HEK human PPARα EC_{50} (μM) (% activity @ 1 μM)[b]
1	Muraglitazar	0.19	0.04 (139%)	0.25	1.41 (107%)
15a	*i*-BuO-C(O)-	7.4	4.65 (6%)	>27.3	5.57 (2%)
17a	*i*-BuO-C(O)-	3.036	1.12 (52%)	1.17	0.028 (104%)
14a	*i*-BuO-C(O)-	0.11	0.074 (95%)	0.255	0.056 (95%)
16a	Benzyl	>27.5	>7.5	>27.5	>7.5
13a	*i*-BuO-C(O)-	4.51	3.86 (37%)	2.56	0.235 (66%)
25a (±)	*i*-BuO-C(O)-	1.25	0.257 (82%)	0.215	0.005 (115%)
22a (±)	*i*-BuO-C(O)-	0.45	0.263 (79%)	0.711	0.044 (101%)
21a (±)	*i*-BuO-C(O)-	>27.3	>7.5	7.62	0.209 (67%)
24a (±)	*i*-BuO-C(O)-	6.03	1.07 (58%)	1.37	0.018 (101%)
31a	*i*-BuO-C(O)-	0.049	0.018 (116%)	0.13	0.006 (82%)
31b	PhO-C(O)-	0.034	0.046 (110%)	0.016	0.004 (87%)
32a (±)	*i*-BuO-C(O)-	3.089	0.49 (75%)	>15	0.58 (48%)
32b (±)	PhO-C(O)-	7.692	1.29 (29%)	8.12	0.17 (62%)
13b	4-Trifluoromethyl-2-pyrimidinyl	1.384	0.644 (65%)	1.328	0.089 (37%)
13c	$PhCH_2O$-C(O)-	4.73	>3.5	>15	4.92 (23%)
13d	*n*-PrO-C(O)-	1.32	0.18 (87%)	0.97	0.04 (85%)
33a (±)	*i*-BuO-C(O)-	0.13	0.009 (132%)	0.861	0.01 (114%)
33b (±)	4-Trifluoromethyl-2-pyrimidinyl	0.287	0.014 (100%)	1.078	0.023 (85%)
33c (±)	$PhCH_2O$-C(O)-	0.133	0.024 (118%)	0.654	0.016 (125%)
33d (±)	*n*-PrO-C(O)-	0.088	0.008 (150%)	0.499	0.008 (109%)

[a] Ref. 19.
[b] Ref. 20.

(**14a**), and the 1,3-oxybenzyl β, γ-unsaturated acids (**33a**–**d**) show potent functional activity at both PPARα and γ.

Conclusions. We have devised efficient and flexible synthetic routes (using as the key step the palladium-catalyzed cross-coupling of nonaflates with organozinc halides) to several series of piperidine and dehydropiperidine carboxylic acids. Analogs from several of these series were identified which show potent agonist activity at both PPARα and γ (e.g. **31b**, **33a**, **b**). One of the dehydropiperidine series (**33**) resulted from a C=C bond migration during base-mediated hydrolysis of the penultimate α, β-unsaturated ester intermediate. The structure of **33** was confirmed through a series of 2D NMR experiments. In the course of these SAR studies, we also identified PPARα-selective agonists (e.g. **17a** and **25a**). These different varieties of analogs should serve as useful leads in our continuing effort to explore the utility of dual PPARα/γ agonists.

Acknowledgment

We thank the BMS Discovery Analytical Sciences Department for analytical support.

Supplementary data

Supplementary data associated with this article can be found, in the online version, at doi:10.1016/j.bmcl.2008.05.014.

References and notes

1. For general reviews on PPARs: Torra, I. P.; Chinetti, G.; Duval, C.; Fruchart, J.-C.; Staels, B. *Curr. Opin. Lipidol.* **2001**, *12*, 245; Evans, A. J.; Krentz, A. J. *Drugs R&D* **1999**, *2*, 75; Sternbach, D. D. *Annu. Rep. Med. Chem.* **2003**, *38*, 71; Cheng, P. T. W.; Mukherjee, R. *Minirev. Med. Chem.* **2005**, *5*, 741.
2. Isseman, I.; Green, S. *Nature (London)* **1990**, *347*, 771; Lee, S. S.; Pineau, T.; Drago, J.; Lee, E. L.; Owens, J. W.; Kroetz, D. L.; Fernandez-Salguero, P. M.; Westphal, H.; Gonzalez, F. J. *Mol. Cell. Biol.* **1995**, *15*, 3012.
3. Staels, B.; Dallongeville, J.; Auwerx, J.; Schoonjans, K.; Leitersdorf, E.; Fruchart, J.-C. *Circulation* **1998**, *98*, 2088.
4. Todd, P. A.; Ward, A. *Drugs* **1988**, *36*, 314–339.
5. Tontonoz, P.; Hu, E.; Spiegelman, B. M. *Cell* **1994**, *79*, 1147.
6. Momose, Y.; Meguro, K.; Ikeda, H.; Hatanka, C.; Oi, S.; Sohda, T. *Chem. Pharm. Bull.* **1991**, *39*, 1440.
7. (a) Willson, T. M.; Brown, P. J.; Sternbach, D. D.; Henke, B. R. *J. Med. Chem* **2000**, *43*, 527; (b) Cantello, B. C. C.; Cawthorne, M. A.; Haigh, D.; Hindley, R. M.; Smith, S. A.; Thurlby, P. *J. Med. Chem* **1994**, *37*, 3977.
8. (a) Devasthale, P. V.; Chen, S.; Jeon, Y.; Qu, F.; Shao, C.; Wang, W.; Zhang, H.; Farrelly, D.; Golla, R.; Grover, G.; Harrity, T.; Ma, Z.; Moore, L.; Ren, J.; Seethala, R.; Cheng, L.; Sleph, P.; Sun, W.; Tieman, A.; Wetterau, J. R.; Doweyko, A.; Chandrasena, G.; Chang, S. Y.; Humphreys, W. G.; Sasseville, V. G.; Biller, S. A.; Ryono, D. E.; Selan, F.; Hariharan, N.; Cheng, P. T. W. *J. Med. Chem.* **2005**, *48*, 2248; (b) Harrity, T.; Farrelly, D.; Tieman, A.; Chu, C.; Kunselman, L.; Gu, L.; Ponticiello, R.; Cap, M.; Qu, F.; Shao, C.; Wang, W.; Zhang, H.; Fenderson, W.; Chen, S.; Devasthale, P.; Jeon, Y.; Seethala, R.; Yang, W.-P.; Ren, J.; Zhou, M.; Ryono, D.; Biller, S.; Mookhtiar, K. A.; Wetterau, J.; Gregg, R.; Cheng, P. T.; Hariharan, N. *Diabetes* **2006**, *55*, 240; (c) Kendall, D. M.; Rubin, C. J.; Mohideen, P.; Ledeine, J.-M.; Belder, R.; Gross, J.; Norwood, P.; O'Mahony, M.; Sall, K.; Sloan, G.; Roberts, A.; Fiedorek, F. T.; DeFronzo, R. A. *Diabetes Care* **2006**, *29*, 1016.
9. (a) Devasthale, P. V.; Chen, S.; Jeon, Y.; Qu, F.; Ryono, D.; Wang, W.; Zhang, H.; Cheng, L.; Farrelly, D.; Golla, R.; Grover, G.; Ma, Z.; Moore, L.; Seethala, R.; Sun,

W.; Doweyko, A. M.; Chandrasena, G.; Sleph, P.; Hariharan, N.; Cheng, P. T. W. *Bioorg. Med. Chem. Lett.* **2007**, *17*, 2312; (b) Wang, W.; Devasthale, P. V.; Farrelly, D.; Gu, L.; Harrity, T.; Cap, M.; Chu, C.; Kunselman, L.; Morgan, N.; Ponticiello, R.; Zebo, R.; Zhang, L.; Locke, K.; Lippy, J.; O'Malley, K.; Hosagrahara, V.; Zhang, L.; Kadiyala, P.; Chang, C.; Muckelbauer, J.; Doweyko, A. M.; Zahler, R.; Ryono, D.; Hariharan, N.; Cheng, P. T. W. *Bioorg. Med. Chem. Lett.* **2008**, *18*, 1939.

10. Cheng, P. T. W.; Chen, S.; Devasthale, P.; Ding, C. Z.; Herpin, T. F.; Wu, S.; Zhang, H.; Wang, W.; Ye, X.-Y. **WO 2004004665 A2**.
11. Bellina, F.; Ciucci, D.; Rossi, R.; Vergamini, P. *Tetrahedron* **1999**, *55*, 2103.
12. 3-(*tert*-Butyldimethylsilyloxy)benzylzinc chloride was prepared freshly from the corresponding benzyl chloride and activated zinc.
13. (a) Olofson, R. A.; Martz, J. T. *J. Org. Chem.* **1984**, *49*, 2081; (b) Campbell, A. L.; Pilipauskas, D. R.; Khanna, I. K.; Rhodes, R. A. *Tetrahedron Lett.* **1987**, *28*, 2331; (c) Yang, B. V.; O'Rourke, D.; Li, J. *Synlett* **1993**, 195.
14. Acid-mediated ester hydrolysis was chosen because our previous experience with the analogous pyrrolidine acid series (e.g. **2**) had shown that base-mediated hydrolysis can result in epimerization at the carbon α to the carboxylic acid (e.g. analogs **22**–**25** in Scheme 3).
15. Compound **27** was synthesized following the procedure in Scheme 2.
16. Schoenberg, A.; Bartoletti, I.; Heck, R. F. *J. Org. Chem.* **1974**, *39*, 3318.
17. The major product from the reaction (a β,γ unsaturated acid) exists as a mixture of rotamers in d_6-DMSO (25 °C), which results in broad signals in the ^{1}H NMR spectrum. To achieve better long range coherence, a set of 2D NMR experiments were performed at elevated temperature (~100 °C), including ^{1}H–^{1}H COSY, ^{1}H–^{13}C HMQC (Heteronuclear Multiple Quantum Coherence), ^{1}H–^{13}C HMBC (Heteronuclear Multiple Bond Connectivity). Each proton and carbon of the product was initially assigned through the use of ^{1}H–^{1}H COSY and HMQC. All proton and carbon assignments were also confirmed using HMBC. For example, in the HMBC spectrum, H-24 (δ 6.73) showed a correlation with C-29 (carbonyl, δ 153.2), while the benzylic protons H-22 (δ 3.36, doublet) showed connectivity with C-23 (δ 115.3), C-24 (δ 123.7), C-28 (δ 40.7), C-16 (δ 116.0), C-17 (δ 141.5), and C-18 (δ 121.9, as shown in Fig. 4). Complete analysis from this set of NMR experiments showed that the structure was unequivocally **33a** rather than **34a**.
18. (a) Jacobsen, P.; Schaumburg, K.; Krogsgaard-Larsen, P. *Acta Chem. Scand. Ser. B* **1980**, *34*, 319; (b) Allan, R. D.; Fong, J. *Aust. J. Chem.* **1983**, *36*, 601.
19. PPARγ and PPARα Binding Assays (Fluorescence-Polarization) were conducted in human PPARα and PPARγ ligand binding domains using a fluorescene-containing oxybenzylglycine derivative as ligand. Binding IC_{50} values (μM) for PPARα and PPARγ were determined by calculating the amount of test ligand required for the half-maximal inhibition of the specific binding of fluorescein-labeled analog of a potent dual PPARα/γ activator to the PPARα or γ LBD, respectively. See: Seethala, R.; Golla, R.; Ma, Z.; Zhang, H.; O'Malley, K.; Lippy, J.; Cheng, L.; Mookhtiar, K.; Farrelly, D.; Zhang, L.; Hariharan, N.; Cheng, P. T. W. *Anal. Biochem.* **2007**, *363*, 263.
20. In vitro PPAR agonist functional assays were performed by transiently transfecting GAL4-hPPARα-LBD or GAL4-hPPARγ-LBD constructs, respectively, into HEK293 cells stably expressing 5× GAL4RE-Luciferase. Data were normalized for efficacy at 1 μM to known agonists. Agonist binding results in an increase in luciferase enzyme activity which can be monitored by measuring luminescence upon cell lysing and the addition of luciferin substrate. EC_{50} values (μM) for PPARα or γ agonist activity were calculated as the concentration of the test ligand (μM) required for the half-maximal fold induction of HEK293 cells. The 'intrinsic activity' of a test ligand is defined as its activity at 1 μM (expressed as a percentage) relative to the activity of the primary standards at 1 μM. Also see Ref. 9a.